Cancer Imaging (2012) **12,** 136–152
DOI: 10.1102/1470-7330.2012.0015

REVIEW

Imaging of sinonasal tumours

Heidi B. Eggesbø

Oslo University Hospital, Oslo, Norway

Corresponding address: Heidi B. Eggesbø, Oslo University Hospital, Oslo, Norway.
Email: h.b.eggesbo@medisin.uio.no

Date accepted for publication 27 January 2012

Abstract

More than 70 benign and malignant sinonasal tumours and tumour-like conditions have been described. However, sinonasal tumours are rare, and sinonasal cancers comprise only 3% of all head and neck cancers and 1% of all malignancies, with a peak incidence in the 5th to 7th decades and with a male preponderance. The early symptoms and imaging findings of sinonasal tumours are similar to rhinosinusitis with runny and stuffy nose, lacrimation and epistaxis and therefore neglected both by the patients and doctors. When late symptoms such as anosmia, visual disturbances, cranial neuropathy (Cn II, IV, V, VI) or facial swelling appear, the patient is referred to sinonasal endoscopy or imaging. At the time of correct diagnosis more than half of the tumours have reached an advanced stage with a poor prognostic outcome. Even if imaging is performed in the early stages, a radiologist inexperienced with sinonasal anatomy and tumour features may easily interpret early signs of a malignant tumour as rhinosinusitis or a lesion that does not require follow-up. This article presents the imaging findings in some of the most common benign and malignant sinonasal tumours, and the TNM classification and staging of sinonasal carcinomas.

Keywords: *Head; neck; sinonasal; neoplasms; computed tomography; magnetic resonance imaging; tumour staging.*

Introduction

More than 70 benign and malignant sinonasal tumours and tumour-like conditions have been described[1]. However, sinonasal tumours are rare, and sinonasal cancers comprise only 3% of all head and neck cancers and 1% of all malignancies, with a peak incidence in the 5th to 7th decades and with a male preponderance.

The early symptoms and imaging findings of sinonasal tumours are similar to rhinosinusitis with runny and stuffy nose, lacrimation and epistaxis and therefore neglected both by the patients and doctors. When late symptoms such as anosmia, visual disturbances, cranial neuropathy (Cn II, IV, V, VI) or facial swelling appear, the patient is referred to sinonasal endoscopy or imaging. At the time of correct diagnosis, more than half of the tumours have reached an advanced stage with a poor prognostic outcome[2,3].

Even if imaging is performed in the early stages, a radiologist inexperienced with sinonasal anatomy and tumour features may easily interpret early signs of a malignant tumour as rhinosinusitis or a lesion that does not require follow-up. Advanced unilateral opacification or bone destruction at imaging should always alert the radiologist.

Endoscopic examination is complementary to imaging and mandatory in order to reveal early stage tumours. Simple polyps may turn out to be malignant, however, there is controversy about whether all polyps and samples removed during endoscopic procedures should undergo histopathologic examination. Alun-Jones et al.[4] found that only 38% of ENT surgeons practiced this routinely in the United Kingdom and suggested that it was unnecessary to send all nasal polyps for histologic examination. Based on 18 cases, Lumsden[5] concluded that every nasal polyp must be submitted for histologic examination. Van den Boer et al.[6] examined 1695 polyp samples and revealed 18 inverted papillomas, 7 squamous cell papillomas, 2 malignant lymphomas, 1 Churg–Strauss syndrome, 1 leiomyosarcoma, 1 Schneiderian papilloma, 2 cases of Wegener granulomatosis, 3 cases of sarcoidosis, 1 papilloma with metaplastic changes and 1 squamous cell carcinoma. They concluded that all the malignant diseases were suspected and that the total cost of finding two unsuspected inverted papillomas was close to 80,000 euros. Hence, routine

histopathologic examination of endoscopic material has little clinical value and it is questionable if this should be performed. Garavello et al.[7] reviewed 2147 cases and came to the same conclusion.

Sinonasal tumours can be of epithelial (carcinomas) or mesenchymal (sarcomas) origin. Epithelial tumours are the most common and originate from the epithelial lining, accessory salivary glands, neuroendocrine tissue and olfactory epithelium. Mesenchymal tumours derive from the supporting tissue.

In sinonasal imaging, the general rules are that benign tumours cause remodelling and thickening of adjacent bone, while malignant tumours destroy the bone. However, there are some malignant tumours that remodel bones rather than destroy it; e.g. sinonasal sarcomas, minor salivary gland carcinomas, extramedullary plasmacytomas, large cell lymphomas, olfactory neuroblastomas and hemangiopericytomas.

The goal of this article is to describe and review the imaging findings in some of the most common benign and malignant sinonasal tumours, and to become familiar with the radiological staging of sinonasal carcinomas.

Imaging

Although some sinonasal tumours have characteristic features and the location of origin can be seen on computed tomography (CT) and magnetic resonance (MR) imaging, only histopathologic examination can provide the correct diagnosis.

CT is the gold standard imaging method for recurrent and chronic rhinosinusitis. In order to evaluate the extent of disease and inflammatory patterns, a low dose protocol (20–40 mAs) without intravenous contrast medium is usually sufficient. However, when using CT for tumour staging and preoperative tumour mapping, higher radiation dose (>50 mAs) and intravenous contrast medium may be needed. CT is the best modality to evaluate bony changes such as cortical erosion, destruction, remodelling, sclerosis and thickening of bone. Reconstruction with both a bone and soft tissue algorithm is important. Volume scanning in the axial plane is crucial to avoid dental filling artefacts into the sinuses as in coronal volume scanning. For optimal evaluation of bony changes, slice thickness as low as 1 mm and reformatting in three planes is mandatory. Key areas to carefully evaluate on CT are the bony orbital walls, cribriform plate, foveolae ethmoidales, posterior wall of the maxillary sinus, pterygopalatine fossa, pterygoid plates, sphenoid sinus, and the posterior table of the frontal sinus.

MR imaging is complementary to CT in order to characterize the soft tissue components of the tumour and to evaluate the extent of tumour invasion beyond the bony sinus walls. The basic MR protocol in imaging sinonasal tumours is unenhanced T1 and T2 with the purpose of discriminating between different soft tissue structures in the tumour and mucous or fluid-filled sinuses. Unenhanced T1 is also optimal for evaluating tumour interruption of the signal void (black) cortical bone or low tumour signal into the high signal fatty bone marrow of the skull base. Around the sinuses, the normal bone may be too thin for proper evaluation by MR[8].

Contrast-enhanced, high-resolution, axial and coronal T1 with or without fat saturation is important for further characterization of soft tissue structures. The short tau inversion recovery (STIR) sequence is useful for lymph node detection and bone marrow oedema. Diffusion weighted (DW) MR imaging is also valuable to distinguish primary tumour and recurrent tumour from surrounding oedema. The proposed optimal *b*-values in sinonasal tumour imaging for pure diffusion are 500 and 1000 in order to calculate the apparent diffusion coefficient (ADC)[9]. MR imaging is also the preferred modality for detecting perivascular and perineural spread as well as orbital and dural tumour invasion[10]. Dural invasion cannot be concluded by linear enhancement alone, but is indicated when dural thickening is more than 5 mm or there is pial enhancement or focal dural nodules[8].

[^{18}F]fluorodeoxyglucose (FDG)-positron emission tomography (PET)/CT imaging is not recommended for routine diagnosis and staging of head and neck cancer in most guidelines[11], however, it has been shown to be useful for imaging of residual and recurrent tumour[12], in monitoring treatment response[11], to measure tumour volume[13], and to select patients who may benefit from oxygenation modifying treatments[14].

For detecting recurrent disease, [^{18}F]FDG-PET/CT is superior to CT and MR imaging, with its high sensitivity, although moderate specificity[15]. Inflammatory side effects from radiation and chemotherapy can cause false-positive FDG uptake, therefore the optimal timing for [^{18}F]FDG-PET/CT has been shown to be more than 3 months after completion of therapy[16,17].

[^{18}F]FDG-PET/CT requires a certain metabolic activity of the tumour in order to accumulate the glucose analogue, [^{18}F]FDG. Most malignant tumours express high metabolic activity with equivalent high FDG uptake. However, there also are benign tumours with high FDG uptake such as pleomorphic adenomas and Warthin tumours of the salivary glands[18]. In contrast, a highly malignant tumour such as adenoid cystic carcinoma of the salivary gland may have low metabolic activity and hence low FDG uptake[19].

Benign tumours

Inverted papillomas and osteomas are the most common benign tumours followed by fibrous dysplasia and neurogenic tumours, e.g. schwannomas.

Osteoma

Osteomas are the most common benign sinonasal tumour and are usually incidental findings at sinus CT. The frontal sinus bone is the most common

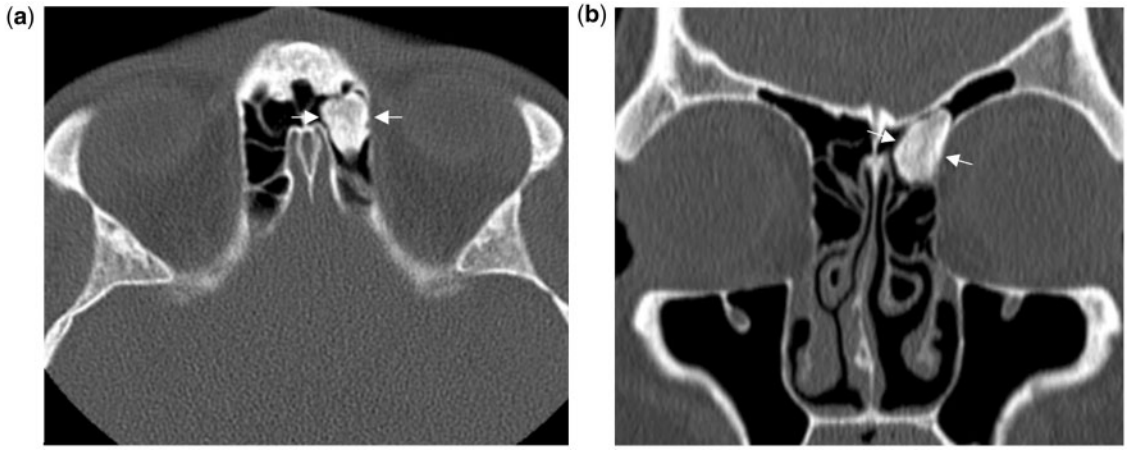

Figure 1 **Osteoma. (a) Axial and (b) coronal CT shows a high density, sclerotic osteoma localized in the left frontal recess (arrows). With time, the osteoma may grow and obstruct mucociliary clearance from the left frontal sinus.**

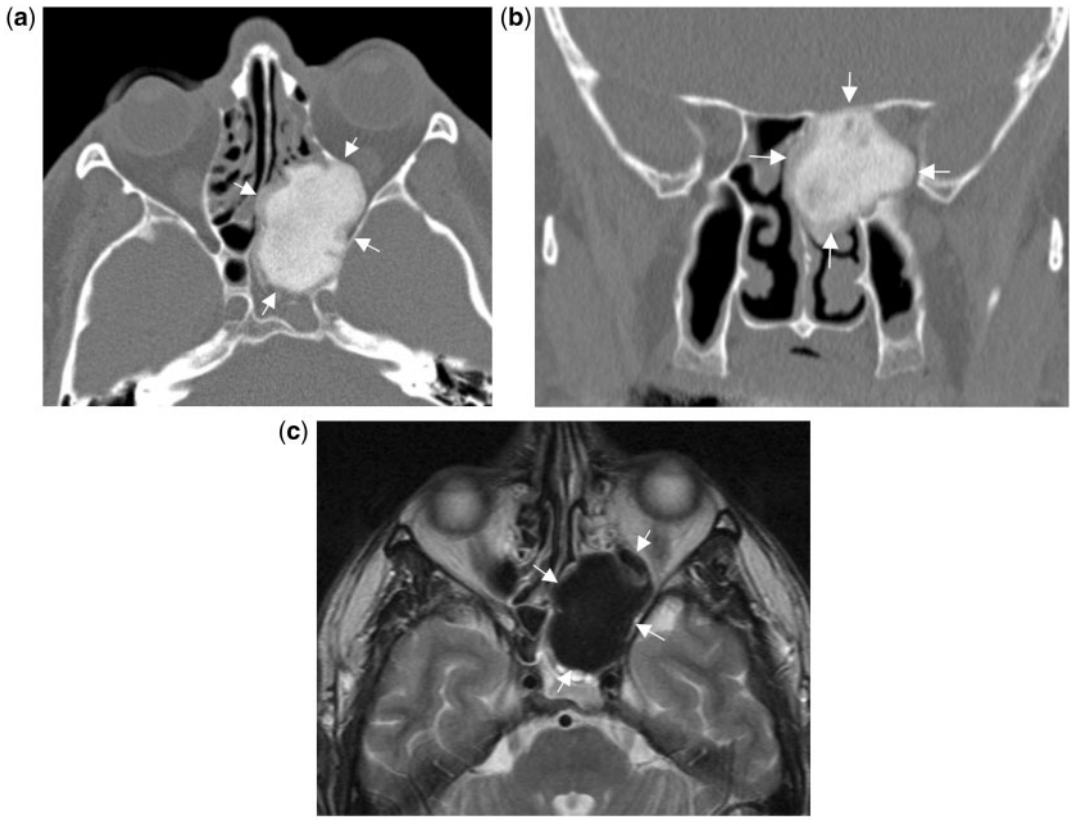

Figure 2 **Osteoma. (a) Axial CT shows a large osteoma with ground-glass appearance (arrows) occupying the left posterior ethmoid sinus. The osteoma bulges into the orbit and displaces the sphenoid sinus posteriorly. (b) axial T2-weighted MR imaging demonstrates the signal void of the osteoma. Notice also the opacified left sphenoid sinus due to obstruction of the sphenoethmoid recess, which is the mucociliary drainage pathway from the sphenoid sinus. The patient presented with exophthalmos, diplopia and headache.**

location (Fig. 1a,b), followed by the ethmoid and maxillary sinus bone[20,21]. Unless growing very large or obstructing the mucociliary drainage pathways, no action is needed for these benign tumours. Multiplanar CT imaging is the best modality to evaluate their relationship to the mucociliary drainage pathways. At CT, osteomas may demonstrate both dense cortical bone and ground-glass appearance (Fig. 2a,b). Osteomas may therefore be difficult to differentiate from fibrous dysplasia.

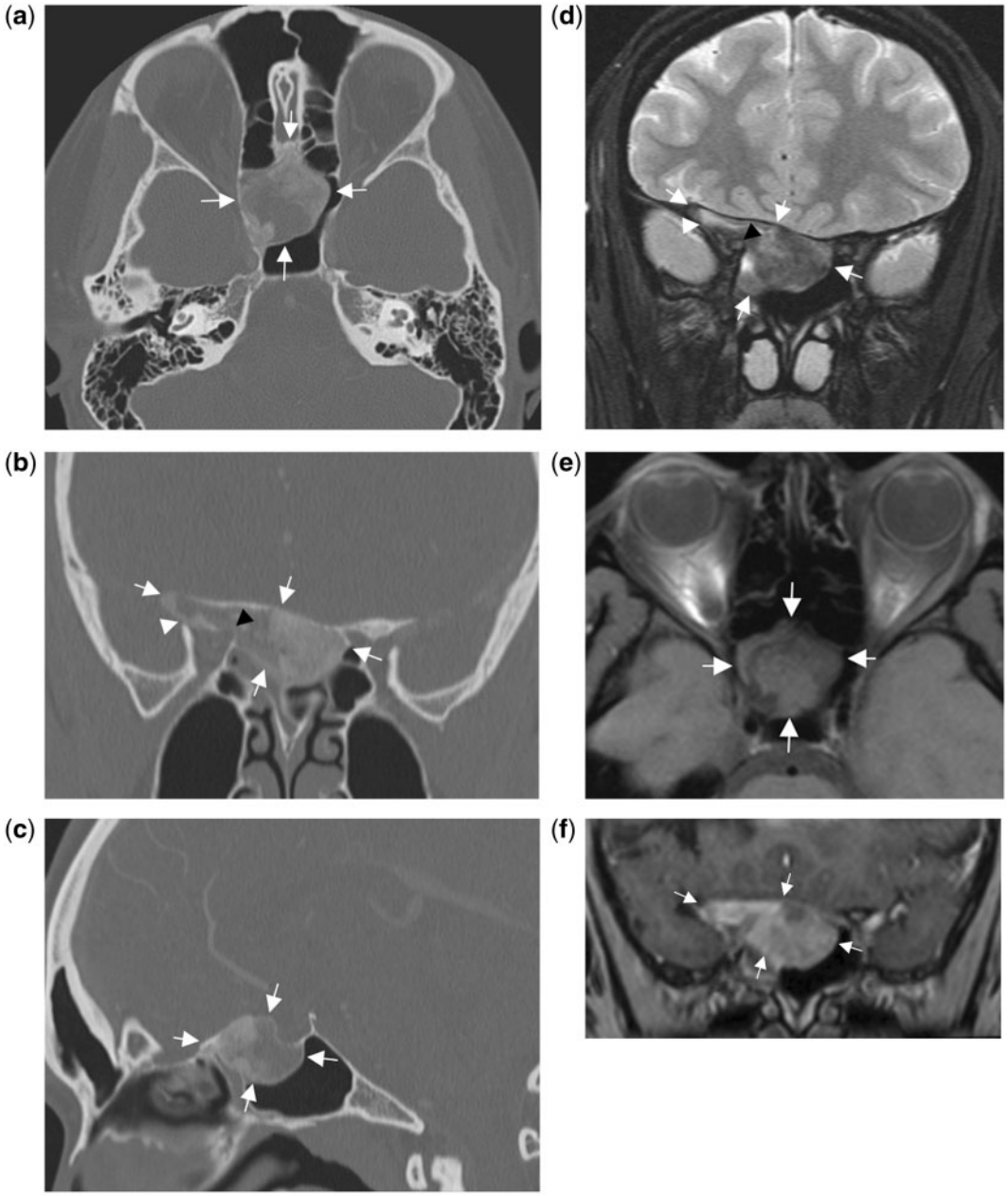

Figure 3 **Fibrous dysplasia. (a) Axial, (b) coronal and (c) sagittal CT demonstrate fibrous dysplasia of the skull base (arrows) involving the sphenoid and posterior ethmoid sinuses. The CT findings are characteristic with partly ground-glass opacification and partly cystic areas. The lesion also involves the right lesser sphenoid wing with narrowing of the optic canal (black arrowhead) and superior orbital fissure (white arrowhead). (d) Axial T2-weighted MR imaging shows heterogeneous signal; (e) axial T1-weighted MR imaging with slightly heterogeneous, intermediate signal; and (f) contrast-enhanced T1-weighted MR imaging demonstrating high signal intensities and enhancement up to the level of fat after intravenous gadolinium. The patient presented with right-sided nervus abducens paralysis, which can be explained by the fact that the abducens nerve is the most medial nerve in the superior orbital fissure and parasellar region (cavernous sinus) and therefore the first nerve to be pushed by this medial lesion.**

Fibrous dysplasia

In fibrous dysplasia, the normal medullary bone is replaced by fibrous tissue that displays a ground-glass appearance on CT (Fig. 3a–c). When seen in the skull base, the paranasal sinuses and their surroundings may also be involved. The radiological findings show three patterns: pagetoid, sclerotic and cystic; the pagetoid form, with bone expansion and mixed areas of sclerosis and cystic areas, is the most common. At CT, the degree of mineralization of the fibrous tissue within the lesion decides the pattern of radiolucency and ground-glass

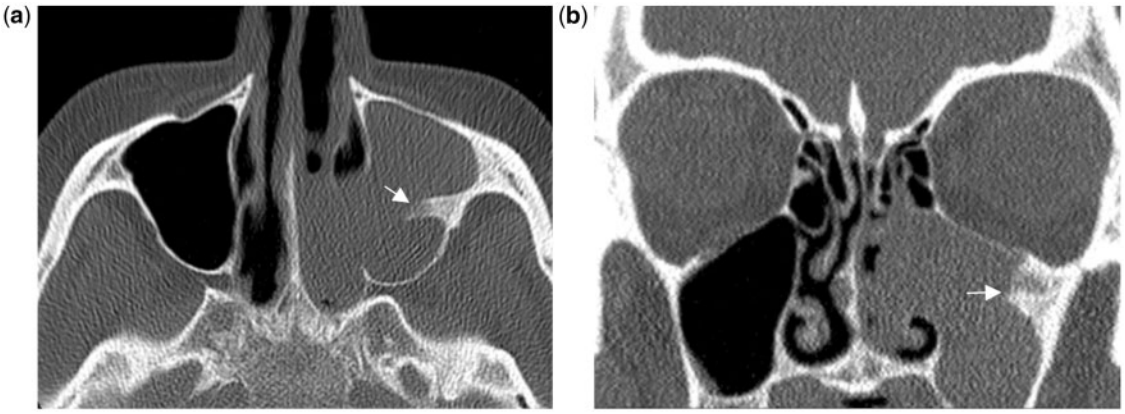

Figure 4 **Inverted papilloma. (a) Axial and (b) coronal CT show total opacification of the left maxillary sinus with medial bulging of the medial sinus wall into the nasal cavity. This was an inverted papilloma with the origin in the left maxillary sinus. A characteristic feature of many inverted papillomas is focal hyperkeratosis (arrows) at the origin of the tumour.**

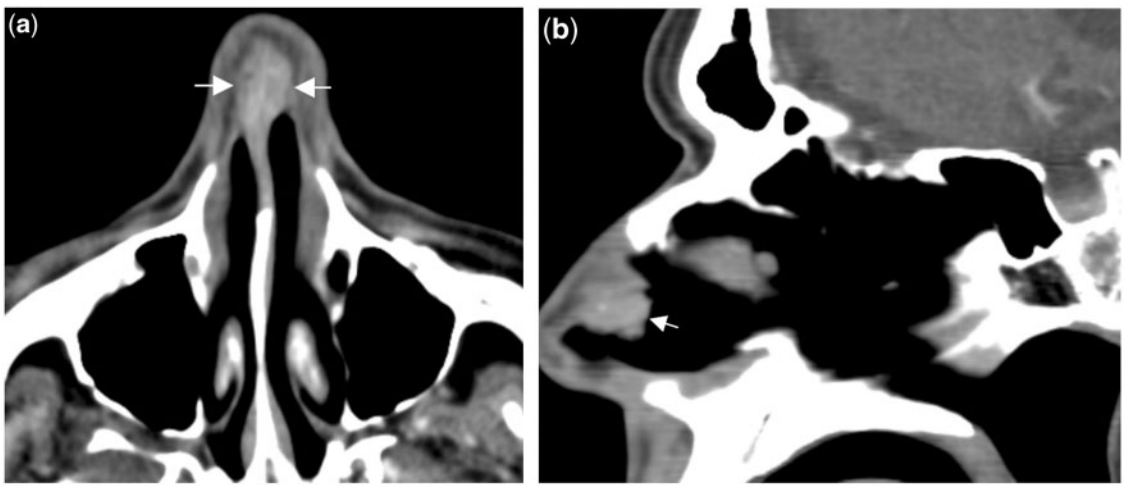

Figure 5 **Exophytic fungiform papilloma. (a) Axial and (b) coronal CT of an exophytic fungiform papilloma, typically found in the mucous membrane of the nasal septum.**

appearance of the lesion[22]. CT usually shows a characteristic pattern, but MR imaging of fibrous dysplasia can be more confusing, because the signals depend on the amount of cystic components and fibrous tissue (Fig. 3d–f). The fibrous tissue is metabolically active and highly vascularized and enhances markedly at contrast-enhanced T1 and therefore can be misinterpreted as a malignant tumour[23].

Sinonasal papilloma

There are three types of sinonasal papillomas: inverted, cylindrical cell and exophytic papillomas. Inverted papillomas (IP) are the second most common benign sinonasal tumour, however they are still rare, accounting for only 0.5–4.0%[24] of primary sinonasal tumours. The histologic feature is mucosal infoldings into the stroma without interrupting the basement membrane. Unlike nasal polyps, IPs are almost always unilateral lesions, and a common CT feature is advanced unilateral ethmomaxillary sinus opacification that remodels or demineralizes the bone and with medial bulging into the nasal septum.

The site of origin of an IP may be detected as focal hyperostosis on the sinus wall at CT (Fig. 4a,b)[25]. Follow-up MR imaging demonstrates the characteristic mucosal infoldings, described as a "convoluted cerebriform pattern" on both T2 and contrast-enhanced T1 sequences[26,27], differentiating tumour from the surrounding mucus and thickened mucosal lining[28].

IPs have potential for both recurrence and malignant transformation. Kim et al.[29] found that 16/228 patients with IP had associated sinonasal carcinoma. They also found a male preponderance (15/16) and that IP

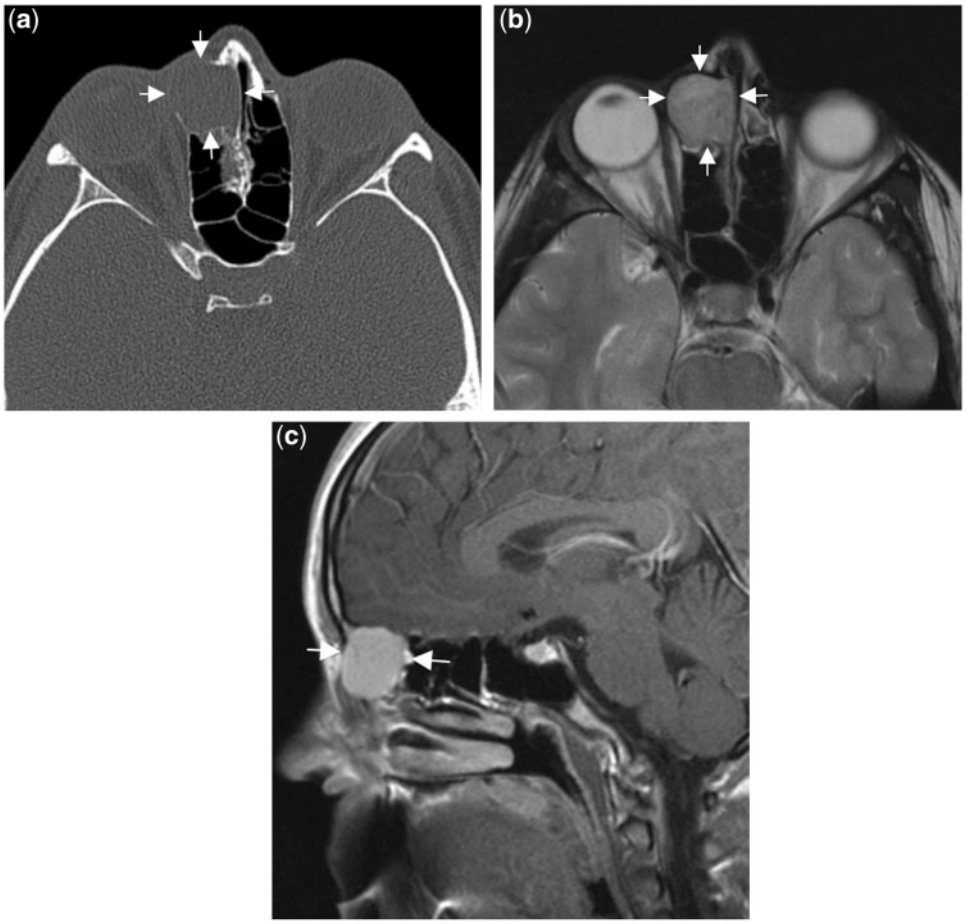

Figure 6 **Schwannoma. (a) Axial CT and (b) axial T2-weighted and (c) sagittal contrast-enhanced T1-weighted MR imaging of a schwannoma (arrows) in the right anterior ethmoid sinus just below the ethmoid roof. Notice the well-delineated expansive growth with remodelling of the surrounding bone and the strong contrast uptake after intravenous contrast injection.**

originating in the frontal sinus or frontal recess was more likely to be associated with malignancy. Moreover, they reported that nearly one-third of the patients developed distant metastases after primary treatment. Increased risk of recurrence has also been reported in cigarette smokers[30].

[^{18}F]FDG-PET/CT imaging has demonstrated high FDG uptake in IP with coexistent carcinoma[31], however the material in this study was small and further studies are required. Several staging systems for IP have been proposed. In 2007, Cannady et al.[32] suggested a staging system that also provides prognostic information, however, there is still no consensus how to stage IP.

Cylindrical cell papillomas behaves clinically as IPs. The exophytic fungiform papilloma originates from the mucosa of the nasal septum (Fig. 5a,b). In contrast to IPs, they rarely undergo malignant transformation[33].

Schwannoma

Sinonasal schwannomas are benign, usually solitary, slow-growing nerve sheath tumours. Although rare, they should be considered in the differential diagnoses. They can arise both from the ophthalmic or maxillary branches of the trigeminal nerve or from autonomic nerves. Olfactory neurons lack Schwann cells, however, the fila olfactoria have a Schwann cell sheath just beyond the level of the olfactory bulb that can give rise to schwannomas[34].

At CT, schwannomas are sharply delineated expansile lesions that remodel bone (Fig. 6a). If large, they can invade vital structures. At MR imaging, they have high signal intensity at T2 (Fig. 6b), and at T1 they are isointense to muscle and surrounded by a low-signal capsule. After intravenous contrast medium, strong homogeneous enhancement is usually seen (Fig. 6c)[35].

Juvenile nasopharyngeal angiofibroma

Juvenile nasopharyngeal angiofibroma (JNA) is a benign, but locally aggressive sinonasal lesion comprising only 0.05% of head and neck tumours and with a reported incidence of 1:5000–1:60,000. These tumours are characterized as a vascular malformation rather than

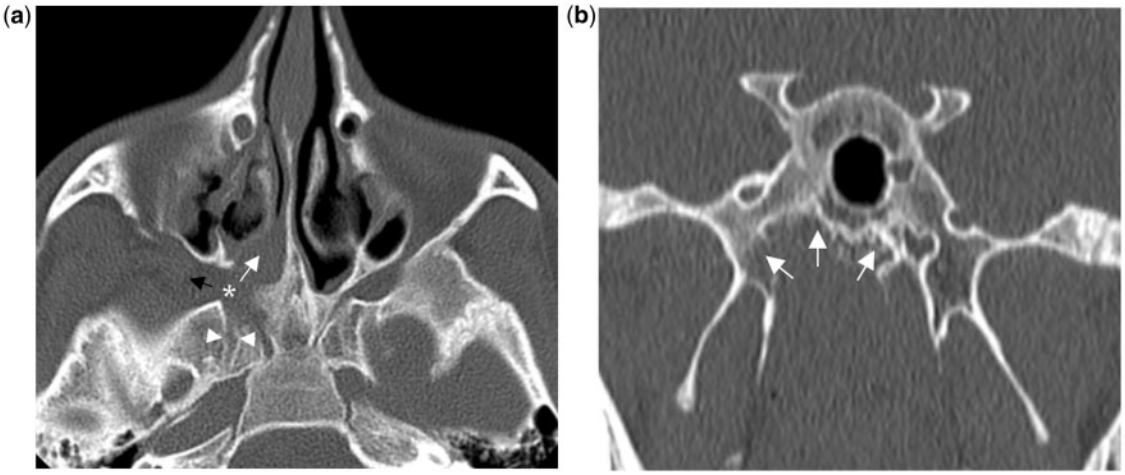

Figure 7 **Juvenile nasopharyngeal angiofibroma. (a) Axial CT shows a tumour that arises from the right pterygoid plate and grows into and widens the pterygopalatine fossa (asterisk). The tumour then grows anteriomedially through the sphenopalatine foramen (white arrow), laterally through the pterygomaxillary fissure (black arrow), and posteriorly into the Vidian canal (arrowheads). (b) Coronal CT demonstrates destruction of the pterygoid plate just posterior to the pterygopalatine fossa.**

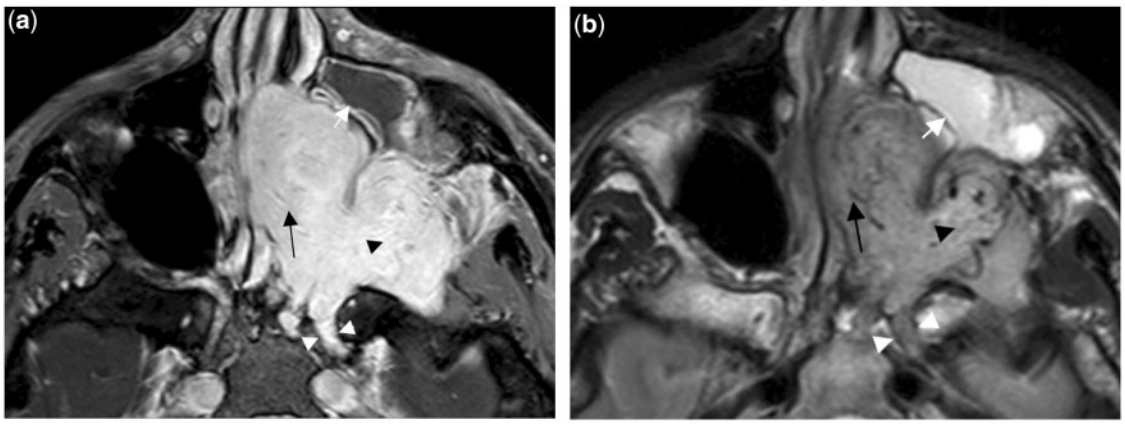

Figure 8 **Juvenile nasopharyngeal angiofibroma in another patient. (a) Axial gradient echo and (b) axial T2-weighted MR imaging of a left-sided tumour growing anteriorly into the nasal cavity (black arrow), dislocating the ipsilateral maxillary sinus anteriorly (white arrow) and growing into the masticator space (black arrowhead). Notice also growth into the broadened Vidian canal (white arrowheads). The rich vascularity of the tumour gives rise to the typical small dotted flow voids.**

a tumour and arise from testosterone-sensitive cells at the pterygoid plates in the pterygopalatine fossa (Fig. 7a,b), and therefore these tumours are only seen in adolescence males. From its origin in the pterygopalatine fossa, the tumour grows in all directions, medially through the sphenopalatine foramen into the nasal cavity and nasopharynx, laterally through the pterygomaxillary fissure, and cranially to the inferior orbital fissure into the orbital apex and then continues through the superior orbital fissure and into the middle cranial fossa[22]. The characteristic imaging pattern at CT is broadening of the pterygopalatine fossa with enlargement of the sphenopalatine foramen medially and the Vidian canal posteriorly. A large tumour may dislocate the posterior maxillary sinus wall anteriorly, the sphenoid sinus upward and the pterygoid plates posteriorly. At MR imaging, due to the high vascularity, the tumour shows typical flow voids and intense enhancement on T1 after gadolinium injection (Fig. 8a,b).

Several staging systems have been proposed for JNA[1]. Recently, due to development of new endoscopic techniques, Snyderman et al.[36] have proposed a new staging system that reflects changes in surgical approach (endonasal) and incorporates prognostic factors such as the route of extension and the extent of vascular supply from the internal carotid artery.

Residual tumours/recurrence rate for JNA is high, ranging from 15% to 50%. Howard et al.[37] postulated that residual tumour in the basisphenoid is the cause, rather than tumour recurrence. Early postoperative contrast-enhanced CT or MR imaging is recommended to detect residual tumour[22,38].

Malignant tumours

Squamous cell carcinoma and adenocarcinoma

Squamous cell carcinoma is most common malignant sinonasal tumour (80%), followed by adenocarcinoma. Both squamous cell carcinoma and adenocarcinoma are associated with occupational exposure. Known agents that increase the risk of sinonasal carcinoma are wood and leather dust, nickel, chromium, welding fumes, isopropyl alcohol, formaldehyde, and arsenic[39]. There are two types of adenocarcinomas, intestinal and non-intestinal; only the former is associated with wood dust exposure. Patients exposed to wood dust are more likely to develop adenocarcinoma than squamous cell carcinoma[40]. In 1968, Acheson et al.[41] described that woodworkers had 500 times increased risk of having sinonasal adenocarcinoma compared with the male population and up to 900 times compared to the population in general.

Carcinomas most often originate from the maxillary sinuses followed by the ethmoid sinuses, nasal vestibule and cavity; carcinomas originating from the sphenoid and frontal sinuses are very rare. Results from endoscopic nasal surgery have recently postulated that the origin of woodworkers' adenocarcinoma is in the olfactory cleft[42].

Staging of sinonasal carcinomas

In order to plan the best treatment and evaluate treatment response, the cancer is staged based on the TNM classification system, where T refers to tumour, N to lymph nodes and M to distant metastases (Tables 1 and 2). Clinical staging is based on information before treatment and used to select proper treatment options; pathologic staging is based on clinical data, surgery and histopathologic evaluation and is used to evaluate the end results (survival)[43]. It is important to bear in mind that the cancer stage does not change with treatment or recurrence. Therefore, one should not go back and change the

Table 2 **Staging of carcinoma of the nasal cavity, ethmoid and maxillary sinus according to the 7th edition of the American Joint Committee on Cancer (AJCC) Cancer Staging Manual**

Stage grouping			
0	Tis	N0	M0
I	T1	N0	M0
II	T2	N0	M0
III	T3	N0	M0
	T1–3	N1	M0
IVA	T1, T2, T3	N2	M0
	T4a	N0, N1, N2	M0
IVB	T4b	Any N	M0
	Any T	N3	M0
IVC	Any T	Any N	M1

Table 1 **TN classification of carcinoma of the nasal cavity, ethmoid and maxillary sinuses according to the 7th edition of the American Joint Committee on Cancer (AJCC) Cancer Staging Manual**

T classification	Maxillary sinus	Nasal cavity and ethmoid sinus	N classification	Lymph node metastases
Tis	Carcinoma in situ	Carcinoma in situ	N0	No regional lymph node metastasis
T1	Tumour limited to the mucosal lining	Tumour limited to the mucosal lining at one subsite	N1	Metastasis in a single ipsilateral lymph node, 3 cm or less in greatest dimension
T2	Bone erosion or destruction limited to the hard palate and middle meatus	Tumour at two subsites or adjacent nasoethmoid site	N2a	Metastasis in a single ipsilateral lymph node 3–6 cm
T3	Bone erosion or destruction of the posterior bone of maxillary sinus, floor and medial bone of orbit. Tumour growth into the pterygoid fossa or ethmoid sinus	Bone erosion of lamina papyracea or floor of orbit, maxillary sinus, palate and cribriform plate	N2b	Metastases in multiple ipsilateral lymph nodes <6 cm
T4a	Tumour growth into the anterior orbit, pterygoid plates, infratemporal fossa, cribriform plate, frontal sinus, sphenoid sinus, or skin of cheek	Tumour growth into the anterior orbit, anterior cranial fossa, pterygoid plates, frontal sinus, sphenoid sinus, or skin of nose or cheek	N2c	Metastasis in bilateral or contralateral lymph nodes <6 cm
T4b	Tumour growth into the orbital apex, dura, brain, middle cranial fossa, cranial nerves other than V_2, nasopharynx and clivus		N3	Metastasis in a lymph node >6 cm

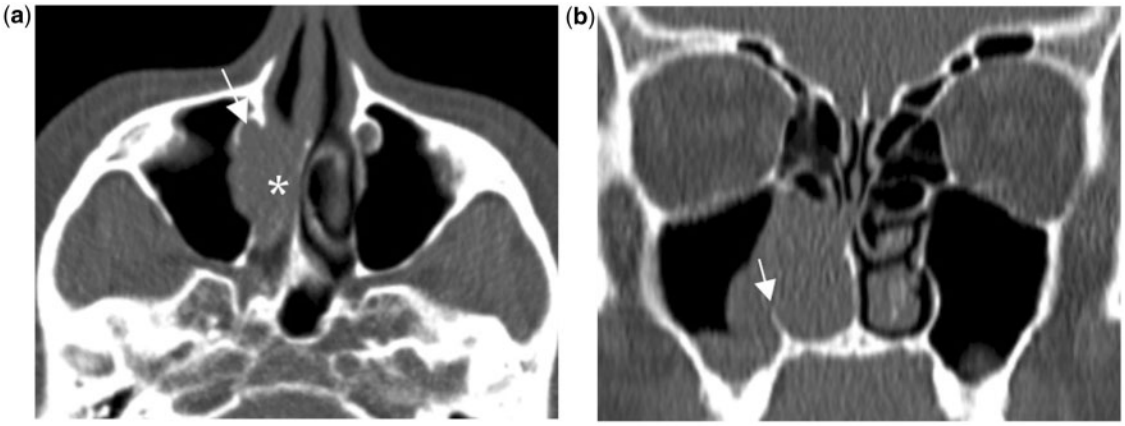

Figure 9 **Maxillary sinus squamous cell carcinoma. (a) Axial CT shows erosion of the lateral nasal wall and lacrimal duct (arrow) and growth into the middle meatus (asterisk) consistent with a T2 cancer. (b) Coronal CT in another patient with a carcinoma mimicking a nasal polyp, however, the lateral nasal wall is eroded (arrow) and the tumour is classified as a T2 cancer.**

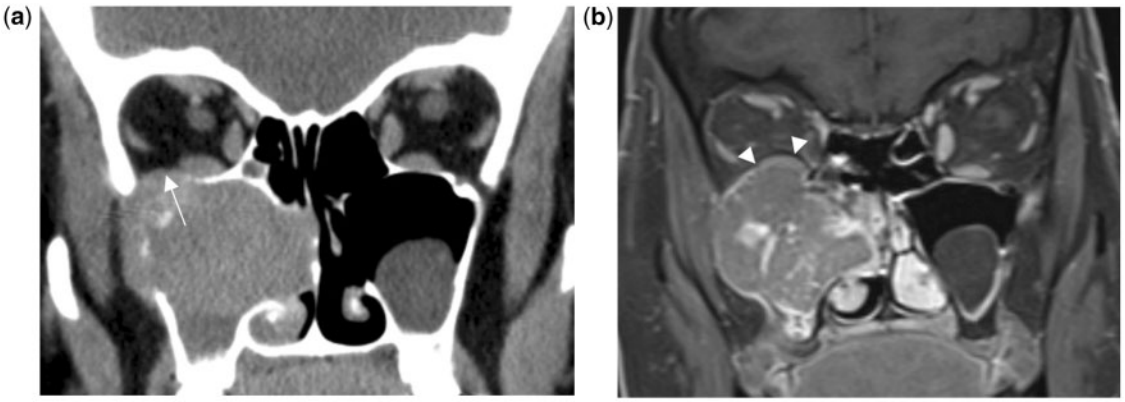

Figure 10 **Maxillary sinus squamous cell carcinoma. (a) Coronal CT and (b) coronal T1-weighted MR imaging with fat saturation after intravenous gadolinium. CT is highly suspicious of tumour growth into the anterior orbit (arrow), classified as T4a cancer. However, the contrast-enhanced T1-weighted MR imaging with fat saturation confirms that the periost acts as a strong barrier against tumour growth into the orbit (arrowheads), hence tumour is classified as a T3 cancer.**

stage of the cancer based on histopathologic staging information[43].

More than half of malignant sinonasal carcinomas are advanced when diagnosed; i.e. classified as T3 or T4 cancers[2,3] (Figs. 9a,b, 10a,b, 11a,b, 12a,b).

Five-year survival for carcinoma is reported to be 50% or less[2,3]. Bhattacharyya[2] reported a three-fold decrease in survival from T1 to T4 cancers, and concluded that early tumour detection was the single most important modifiable treatment factor. Another important factor is tumour site; carcinomas originating in the nasal cavity have a better prognosis than carcinomas in the ethmoid and maxillary sinuses[3].

Sinonasal carcinoma mainly metastasizes to level I, II and III lymph nodes and retropharyngeal lymph nodes; metastases to the tonsillar region are most commonly seen when the posterior ethmoid and sphenoid sinuses are involved. Cantù et al.[44] found that lymph node metastases were rare, and when present, the prognostic factors were low with 5-year survival of 17% for maxillary sinus and 0% for ethmoid sinus carcinomas. The highest rate of lymph node metastases was found in T2 squamous cell carcinoma that involved the floor of the maxillary sinus.

In order to delineate the limits of resectability of a tumour in the maxillary sinus, in 1930, Ohngren described a line (the Ohngren line) from the medial canthus of the eye to the angle of the mandible; tumour posterior to the Ohngren line was considered to be an unresectable tumour (Fig. 13). With advances in surgical techniques, this line of resectability has been moved further posteriorly and only when the tumour grows into the orbital apex, dura, brain, middle cranial fossa, cranial nerves other than V_2, nasopharynx and clivus, is surgery no longer a treatment option.

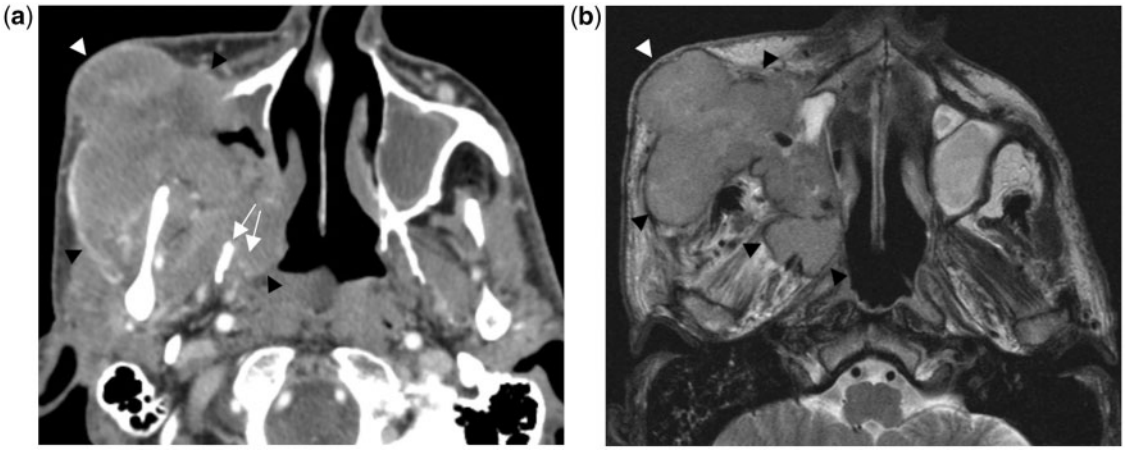

Figure 11 **Maxillary sinus squamous cell carcinoma. (a) Axial CT and (b) T2-weighted MR imaging demonstrate a tumour (black arrowheads) extending to the skin of the cheek (white arrowhead) classified as T4a cancer. The bony erosion of the lateral maxillary sinus wall and the pterygoid plates (arrows) are better visualized using CT; the extension of the tumour and distinction from obstructed fluid-filled sinuses and surrounding oedematous soft tissue are best evaluated using MR imaging.**

Figure 12 **Ethmoid sinus adenocarcinoma. (a) Coronal CT shows opacification of the left nasal cavity, anterior ethmoid sinus and frontal recess. The clue to a malignant process is the erosion of the lateral lamella (arrow). (b) Contrast-enhanced coronal CT shows an intracranial component (arrowheads) verified at (c) coronal contrast-enhanced T1-weighted MR imaging. There is no meningeal enhancement due to the dural barrier. The tumour also respects the orbit and was classified as a T3 cancer.**

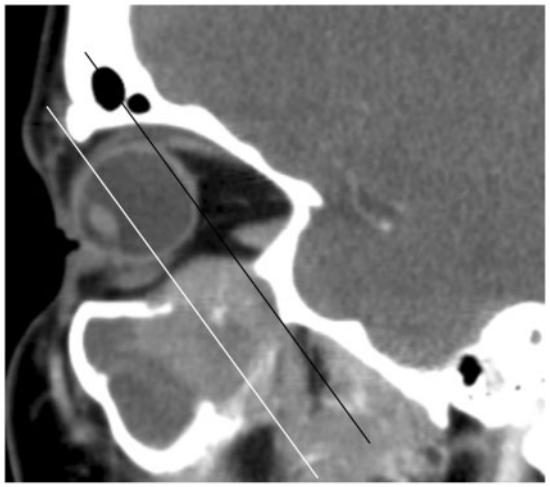

Figure 13 **The Ohngren line. Sagittal CT shows a squamous cell carcinoma with the origin in the posterior maxillary sinus. The white line refers to the Ohngren line, where cancer posterior to this line was previously considered unresectable. The posterior black line is the border between a T4a and a T4b cancer (AJCC 7th edition). T4a is now defined as moderately advanced cancer and T4b as very advanced cancer. This tumour erodes the posterior maxillary wall and bulges into the orbital apex, but the periost is intact consistent with a T3 cancer.**

In the 7th edition of the American Joint Committee on Cancer (AJCC) staging manual, the terms resectable and unresectable have been replaced with moderately advanced and very advanced, respectively[43], and the T4 sinonasal carcinomas have been divided into T4a (moderately advanced local disease) and T4b (very advanced local disease). According to these changes, the previous clinical stage IV has been split into stage IVA (moderately advanced local/regional disease), stage IVB (very advanced local/regional disease), and stage IVC (distant metastatic disease)[43].

Chondrosarcoma

Chondrosarcoma is a malignant cartilage tumour that is the second most frequent primary malignant tumour of bone and the most common sarcoma affecting the paranasal sinuses. When appearing in the skull base, the sinonasal tract is usually involved when the tumour presents with symptoms. At CT, the tumour is seen as a multilobulated, heterogeneous lesion consisting of a chondroid matrix with peripheral and scattered central calcifications. The chondroid matrix has high water content and therefore displays with lower attenuation compared with muscle (Fig. 14a). Using MR imaging, the high water content of the chondroid matrix presents with high signal on T2 (Fig. 14b) and low signal on T1;

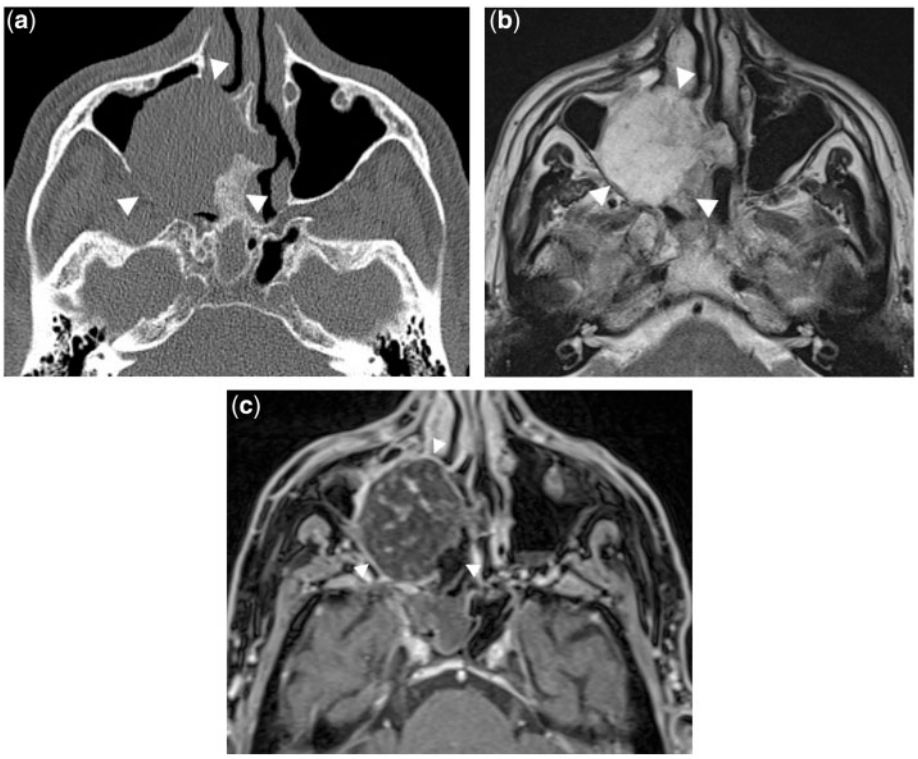

Figure 14 **Chondrosarcoma. (a) Axial CT of a well-delineated tumour of the maxillary and ethmoid sinuses, and nasal cavity (arrowheads). (b) Axial T2-weighted MR imaging shows high signal of the chondroid matrix with sparse, low signal areas of septa and calcifications. (c) Contrast-enhanced T1-weighted MR imaging shows contrast uptake in the septa and low signal in the surrounding chondroid matrix.**

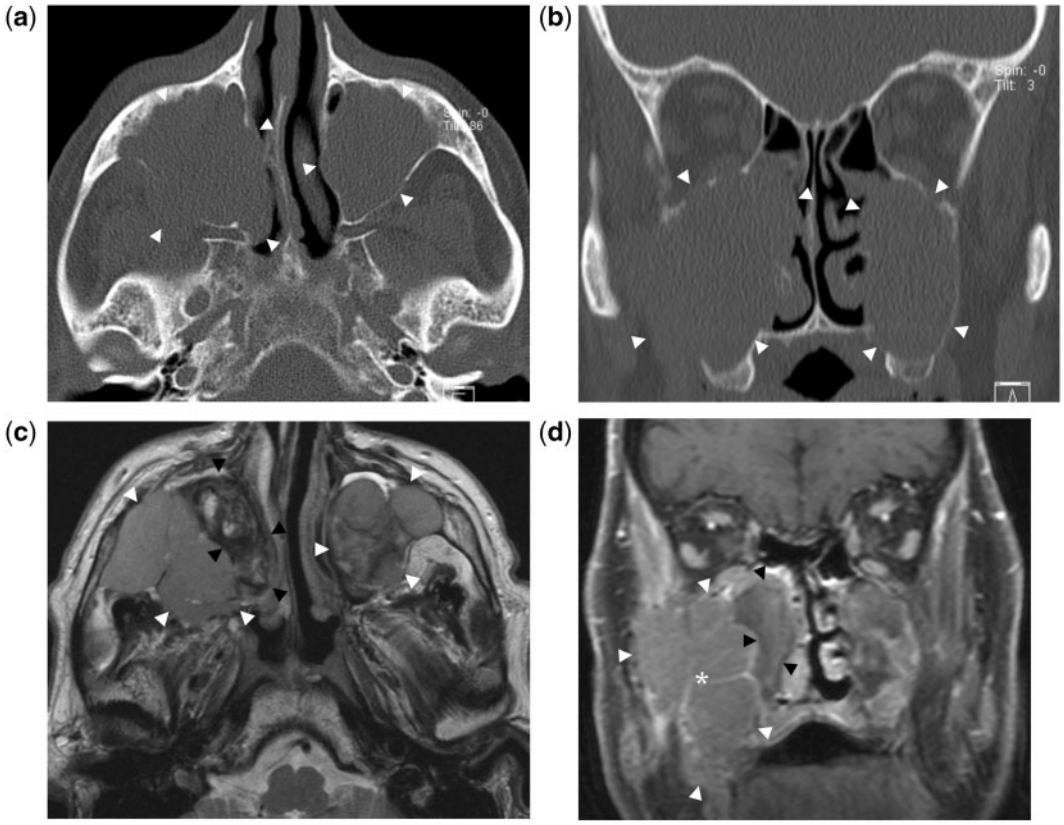

Figure 15 **B-cell lymphoma. (a) Axial and (b) coronal CT demonstrate advanced opacification of both maxillary sinuses (white arrowheads). At MR imaging, (c) axial T2 and (d) coronal T1 after gadolinium injection demonstrate a large, bulky tumour on both sides of the maxillary sinus walls. MR imaging shows that the medial part of the right maxillary sinus contains mucus (black arrowheads) and that the epicentre of the tumour masses (asterisk) is close to the lateral sinus wall, which is a common finding in sinonasal B-cell lymphomas.**

Figure 16 **Adenoid cystic carcinoma. Coronal CT mimics the features of a simple polyp filling the left nasal cavity (arrowheads) and slightly remodelling the bones.**

calcifications of the chondroid matrix cause signal voids at all sequences. Also the septum shows low signal at both T1 and T2. After injection of contrast medium, both CT and MR imaging demonstrate a heterogeneous pattern due to septal enhancement, but the avascular chondroid matrix is unchanged (Fig. 14c)[45].

Lymphoma

Lymphoma is a cancer that arises in the nodal and extranodal lymphoid tissue. Lymphomas have been named Hodgkin lymphoma (HL) and non-Hodgkin lymphoma (NHL) after Thomas Hodgkin who first described lymphoma in 1932. Since then, more than 70 different forms of lymphoma have been listed by the World Health Organization[46]. The term NHL has been replaced by the group of dominating cell types into B, T and natural killer (NK) cell lymphomas. Lymphomas in the sinonasal cavities have worse outcome than lymphomas in other regions. B-cell lymphomas are most common in the maxillary sinus and have a better prognosis than T-cell lymphomas, which more often originate from the nasal septum. Sinonasal lymphomas are more common in Asia than in the western world.

The clinical presentation depends on the histologic type and sinonasal location. Early symptoms are nasal discharge, obstruction, and epistaxis, mimicking rhinosinusitis[47]. Therefore, the clue to the diagnosis is usually

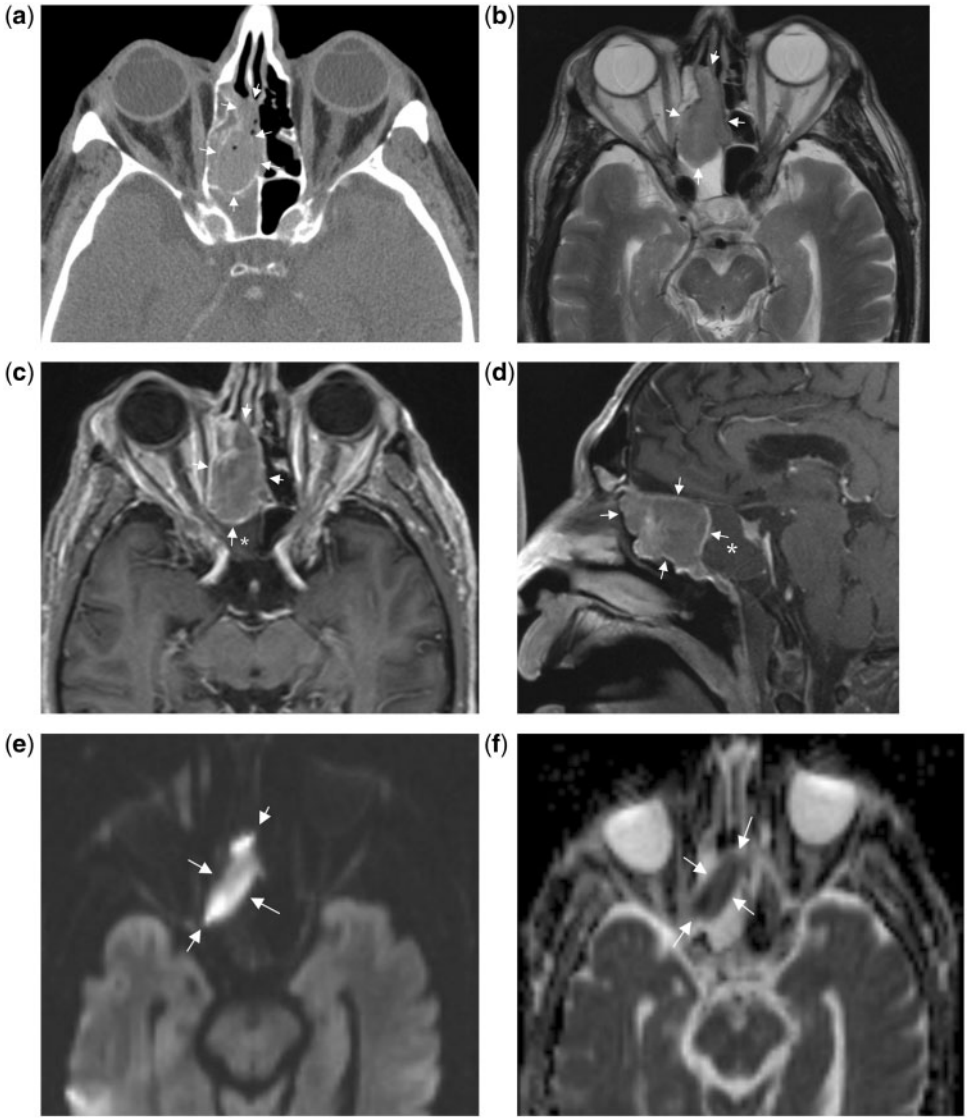

Figure 17 **Olfactory neuroblastoma. (a) Axial CT shows an expansile soft tissue mass remodelling the ethmoid bones (arrows). At MR imaging, (b) axial T2 shows a well-delineated tumour with homogeneous low signal (arrows) with surrounding high signal sinonasal fluid. (c) Axial T1 and (d) sagittal T1 after intravenous gadolinium delineate the tumour (arrows) from the adjacent dark signal fluid-filled sphenoid sinus (asterisk). The sagittal image demonstrates the close relationship between the tumour and the ethmoid roof. (e) Axial diffusion-weighted imaging with $b = 1000$ and (f) ADC map shows the characteristic low diffusion signal intensities (arrows) of a malignant tumour.**

the late symptoms such as non-healing ulcers and septum and bone destruction. Both unilateral and bilateral presentations are reported[48]. The spectrum of biological behaviours of lymphoma range from chronic indolent tumours present for years before diagnosis, to rapidly growing tumours that double in size over days. The chronic indolent lymphoma is rare and may mimic invasive fungal sinusitis in its presentation.

At CT and MR imaging, lymphomas can present with diffuse tumour infiltration along the walls of the nasal cavity or as large bulky masses on both sides of the sinus wall, with remodelling or erosion of the adjacent bone (Fig. 15a–d). Lymphomas are isodense to muscle at CT, and at MR imaging, the signal is isointense to muscle on T1 and moderate to high on T2. Both at CT and MR imaging, the contrast enhancement of lymphomas can be variable and not discriminated from other malignancies, e.g. squamous cell carcinoma[49].

The value of [^{18}F]FDG-PET/CT has been shown for nasal lymphomas, but not for paranasal sinus lymphomas[50]. Lymphomas may spread to the meninges and central nervous system disease occurs in about 5% of patients with NHL[51].

Salivary gland tumours

Small salivary glands are distributed along the sinonasal tract and number more than several hundreds, and all

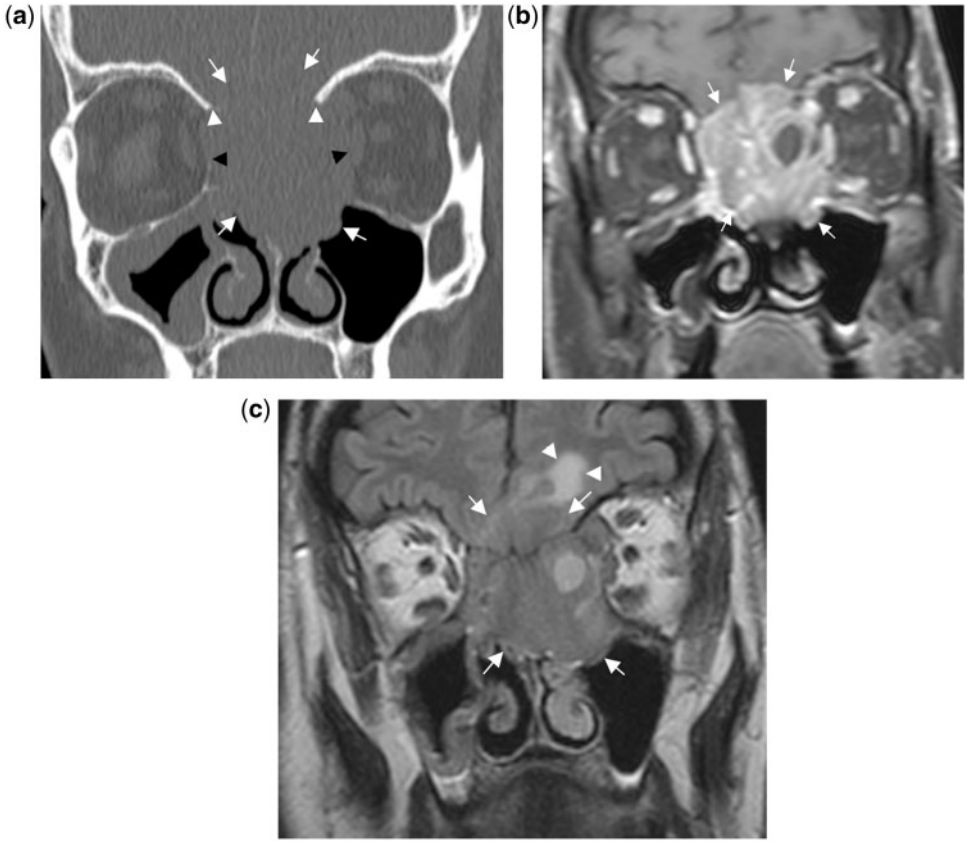

Figure 18 **Sinonasal undifferentiated carcinoma. (a) Coronal CT, (b) coronal T1-weighted MR imaging with fat saturation after intravenous gadolinium and (c) coronal flair sequence demonstrating a highly aggressive tumour (arrows) with destruction of the lamina papyracea (black arrowheads) and the ethmoid roof (white arrowheads). The tumour enhances strongly after intravenous contrast medium and the fluid attenuated inversion recovery sequence demonstrates brain oedema (arrowheads). Immunohistologic examination concluded with SNUC.**

types of salivary gland tumours can therefore be found in the nasal cavity and paranasal sinuses. Of these, adenoid cystic carcinoma (ACC) is the most common with its origin usually in the maxillary or ethmoid sinuses. Low-grade ACC may present as an ethmoid polyp that remodels bone and mimics a simple polyp (Fig. 16) at both CT and MR imaging; high-grade ACC may present as a large irregular mass with bone destruction and irregular density and signal at CT and MR imaging. ACC is also well known for its predisposition to perineural spread along the cranial nerves that can proceed into the skull base. In order to map perineural spread, MR imaging with intravenous contrast injection is mandatory. The recurrence rate is reported to more than 60% when the tumour originates in the sinonasal tract, and tumour recurrence has been reported as long as 15 years after treatment[52]. The value of [^{18}F]FDG-PET/CT in ACC is limited due to low metabolic activity and therefore low FDG uptake[19].

Neuroendocrine tumours

Four histologic phenotypes of neuroendocrine tumours have been described: the olfactory neuroblastoma (ONB) (also referred to as esthesioneuroblastoma), sinonasal neuroendocrine carcinoma (SNEC), sinonasal undifferentiated carcinoma (SNUC), and small cell undifferentiated carcinoma (SmCC)[53]. Of these four aggressive tumours, the ONB is the most differentiated. ONB originates in the superior nasal fossa and shows a bimodal age distribution with a peak in the 20th and 60th decades. Different staging systems have been proposed and the most useful to date has been the Kadish staging system, where tumour confined to the nasal cavity (stage A) has the best prognosis. Tumour in the nasal cavity and one or more paranasal sinuses (stage B) and tumour extending beyond the nasal cavity and paranasal sinuses (stage C) have poorer prognosis. The recurrence rate after extended lateral rhinotomy is reported to be as high as 50% and the 5-year survival rate for all stages is 70%[1]. At CT and MR imaging ONB may present as a homogeneous, solitary nasal polyp that remodels rather than destroys the bone (Fig. 17a–f). The MR signal is intermediate on both T1 and T2, and after intravenous contrast medium, there is intermediate to high enhancement of the tumour. SNEC and SNUC (Fig. 18a–c) were first known as distinct entities after the 1980s[54].

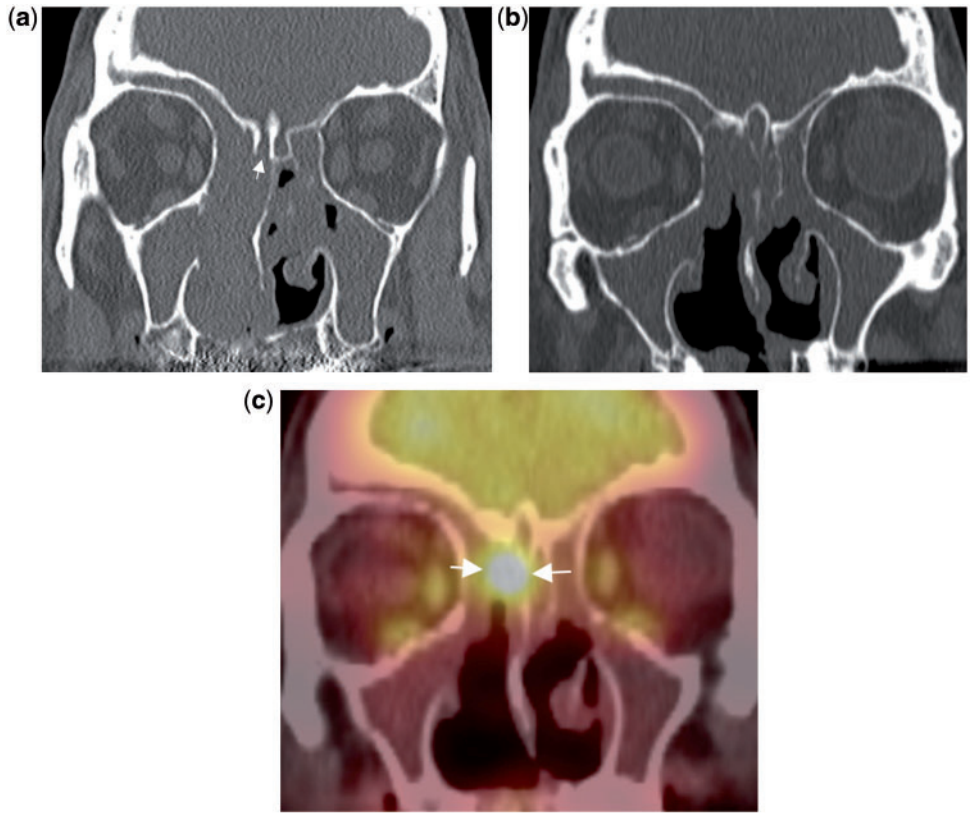

Figure 19 **Mucosal malignant melanoma. (a) Coronal CT demonstrates advanced sinonasal opacification with erosion of the right olfactory fossa and lateral lamella (arrow) due to MMM. (b) Coronal CT after surgical treatment still shows bilateral advanced opacification and (c) coronal [^{18}F]FDG-PET/CT confirmed residual or recurrent tumour in the right anterior ethmoid sinus (arrow). Notice also physiologic FDG uptake in the brain and in the lateral and inferior eye muscles.**

The CT and MR features of these aggressive tumours are bone erosion similar to that of squamous cell carcinoma, and the correct diagnosis can only be done by immunohistologic examination[53,55,56].

Mucosal malignant melanoma

Sinonasal mucosal malignant melanoma (MMM) accounts for 1% of all melanomas in western countries but up to 11% of melanomas in Japan. The nasal septum is the most common origin. MMM is an aggressive tumour with up to 64% recurrence 1 year after surgery and overall 5-year survival of less than 30%[57]. At CT, MMM can be seen as a polypoid lesion in the nasal cavity that remodels the surrounding bone, but bony erosion may also be seen. After injection of contrast medium, there is strong enhancement due to the rich vascular network. At MR imaging, the lesion is homogeneous, but high T1 signal may sometimes be seen due to bleeding or paramagnetic melanin in the tumour. In this case, the MMM may characteristically present with low T2 and high T1 signals. TNM classification and staging for MMM have been included in the AJCC 7th edition. However, so far, tumour staging has shown no impact on the poor prognosis with overall 5-year survival less than 25%. For early stage disease, 5-year survival is around 40%[58]. [^{18}F]FDG-PET/CT has been shown to be useful in evaluating residual or recurrent MMM (Fig. 19 a–c)[59].

References

[1] Blount A, Riley KO, Woodworth BA. Juvenile nasopharyngeal angiofibroma. Otolaryngol Clin North Am 2011; 44: 989–1004, ix. doi:10.1016/j.otc.2011.06.003.

[2] Bhattacharyya N. Factors affecting survival in maxillary sinus cancer. J Oral Maxillofac Surg 2003; 61: 1016–1021. doi:10.1016/S0278-2391(03)00313-6.

[3] Thorup C, Sebbesen L, Danø H, et al. Carcinoma of the nasal cavity and paranasal sinuses in Denmark 1995–2004. Acta Oncol 2010; 49: 389–394. doi:10.3109/02841860903428176.

[4] Alun-Jones T, Hill J, Leighton SE, Morrissey MS. Is routine histological examination of nasal polyps justified? Clin Otolaryngol Allied Sci 1990; 15: 217–219.

[5] Lumsden A, Wilson JA, McLaren K, Maran AG. Unusual polypoidal tumours of the nasal cavity: a clinicopathological review of 18 cases. Clin Otolaryngol Allied Sci 1986; 11: 31–36.

[6] van den Boer C, Brutel G, de Vries N. Is routine histopathological examination of FESS material useful? Eur Arch Otorhinolaryngol 2010; 267: 381–384. doi:10.1007/s00405-009-1097-2.

[7] Garavello W, Gaini RM. Histopathology of routine nasal polypectomy specimens: a review of 2,147 cases. Laryngoscope 2005; 115: 1866–1868. doi:10.1097/01.mlg.0000177075.09594.90.

[8] Casselman JW. The skull base: tumoral lesions. Eur Radiol 2005; 15: 534–542. doi:10.1007/s00330-004-2532-9.
[9] Sasaki M, Eida S, Sumi M, Nakamura T. Apparent diffusion coefficient mapping for sinonasal diseases: differentiation of benign and malignant lesions. AJNR Am J Neuroradiol 2011; 32: 1100–1106. doi:10.3174/ajnr.A2434.
[10] Maroldi R, Farina D, Borghesi A, Marconi A, Gatti E. Perineural tumor spread. Neuroimaging Clin North Am 2008; 18: 413–429, xi. doi:10.1016/j.nic.2008.01.001.
[11] Bussink J, van Herpen CML, Kaanders JHAM, Oyen WJG. PET-CT for response assessment and treatment adaptation in head and neck cancer. Lancet Oncol 2010; 11: 661–669. doi:10.1016/S1470-2045(09)70353-5.
[12] Fukui MB, Blodgett TM, Snyderman CH, et al. Combined PET-CT in the head and neck: part 2. Diagnostic uses and pitfalls of oncologic imaging. Radiographics 2005; 25: 913–930. doi:10.1148/rg.254045136.
[13] Daisne J-F, Duprez T, Weynand B, et al. Tumor volume in pharyngolaryngeal squamous cell carcinoma: comparison at CT, MR imaging, and FDG PET and validation with surgical specimen. Radiology 2004; 233: 93–100. doi:10.1148/radiol.2331030660.
[14] Kaanders JHAM, Wijffels KIEM, Marres HAM, et al. Pimonidazole binding and tumor vascularity predict for treatment outcome in head and neck cancer. Cancer Res 2002; 62: 7066–7074.
[15] Wong RJ. Current status of FDG-PET for head and neck cancer. J Surg Oncol 2008; 97: 649–652. doi:10.1002/jso.21018.
[16] Greven KM, Williams DW, 3rd. McGuirt WF, Sr. et al. Serial positron emission tomography scans following radiation therapy of patients with head and neck cancer. Head Neck 2001; 23: 942–946. doi:10.1002/hed.1136.
[17] Lonneux M, Lawson G, Ide C, Bausart R, Remacle M, Pauwels S. Positron emission tomography with fluorodeoxyglucose for suspected head and neck tumor recurrence in the symptomatic patient. Laryngoscope 2000; 110: 1493–1497. doi:10.1097/00005537-200009000-00016.
[18] Okamura T, Kawabe J, Koyama K, et al. Fluorine-18 fluorodeoxyglucose positron emission tomography imaging of parotid mass lesions. Acta Otolaryngol 1998; 538(Suppl): 209–213.
[19] Jeong HS, Chung MK, Son YI, et al. Role of ^{18}F-FDG PET/CT in management of high-grade salivary gland malignancies. J Nucl Med 2007; 48: 1237–1244. doi:10.2967/jnumed.107.041350.
[20] Eller R, Sillers M. Common fibro-osseous lesions of the paranasal sinuses. Otolaryngol Clin North Am 2006; 39: 585–600, x. doi:10.1016/j.otc.2006.01.013.
[21] McHugh JB, Mukherji SK, Lucas DR. Sino-orbital osteoma: a clinicopathologic study of 45 surgically treated cases with emphasis on tumors with osteoblastoma-like features. Arch Pathol Lab Med 2009; 133: 1587–1593.
[22] Maroldi R, Ravanelli M, Borghesi A, Farina D. Paranasal sinus imaging. Eur J Radiol 2008; 66: 372–386. doi:10.1016/j.ejrad.2008.01.059.
[23] Chong VFH, Khoo JBK, Fan Y-F. Imaging of the nasopharynx and skull base. Neuroimaging Clin North Am 2004; 14: 695–719. doi:10.1016/j.nic.2004.07.014.
[24] Melroy CT, Senior BA. Benign sinonasal neoplasms: a focus on inverting papilloma. Otolaryngol Clin North Am 2006; 39: 601–617, x. doi:10.1016/j.otc.2006.01.005.
[25] Lee DK, Chung SK, Dhong H-J, Kim HY, Kim H-J, Bok KH. Focal hyperostosis on CT of sinonasal inverted papilloma as a predictor of tumor origin. AJNR Am J Neuroradiol 2007; 28: 618–621.
[26] Ojiri H, Ujita M, Tada S, Fukuda K. Potentially distinctive features of sinonasal inverted papilloma on MR imaging. AJR Am J Roentgenol 2000; 175: 465–468.
[27] Maroldi R, Farina D, Palvarini L, Lombardi D, Tomenzoli D, Nicolai P. Magnetic resonance imaging findings of inverted papilloma: differential diagnosis with malignant sinonasal tumors. Am J Rhinol 2004; 18: 305–310.
[28] Sham CL, King AD, van Hasselt A, Tong MCF. The roles and limitations of computed tomography in the preoperative assessment of sinonasal inverted papillomas. Am J Rhinol 2008; 22: 144–150. doi:10.2500/ajr.2008.22.3142.
[29] Kim K, Kim D, Koo Y, et al. Sinonasal carcinoma associated with inverted papilloma: a report of 16 cases. J Craniomaxillofac Surg 2011; doi:10.1016/j.jcms.2011.07.007.
[30] Moon IJ, Lee DY, Suh M-W, et al. Cigarette smoking increases risk of recurrence for sinonasal inverted papilloma. Am J Rhinol Allergy 2010; 24: 325–329. doi:10.2500/ajra.2010.24.3510.
[31] Jeon TY, Kim H-J, Choi JY, et al. ^{18}F-FDG PET/CT findings of sinonasal inverted papilloma with or without coexistent malignancy: comparison with MR imaging findings in eight patients. Neuroradiology 2009; 51: 265–271. doi:10.1007/s00234-009-0510-2.
[32] Cannady SB, Batra PS, Sautter NB, Roh H-J, Citardi MJ. New staging system for sinonasal inverted papilloma in the endoscopic era. Laryngoscope 2007; 117: 1283–1287. doi:10.1097/MLG.0b013e31803330f1.
[33] Som PM, Curtin HD. Head and neck imaging. 2 volume set. 5th ed. St Louis, MO: Mosby; 2011.
[34] Murakami M, Tsukahara T, Hatano T, Nakakuki T, Ogino E, Aoyama T. Olfactory groove schwannoma–case report. Neurol Medico-Chirurg 2004; 44: 191–194. doi:10.2176/nmc.44.191.
[35] Lemmerling M, Moerman M, Govaere F, Praet M, Kunnen M, Vermeersch H. Schwannoma of the tip of the nose: MRI. Neuroradiology 1998; 40: 264–266. doi:10.1007/s002340050582.
[36] Snyderman CH, Pant H, Carrau RL, Gardner P. A new endoscopic staging system for angiofibromas. Arch Otolaryngol Head Neck Surg 2010; 136: 588–594. doi:10.1001/archoto.2010.83.
[37] Howard DJ, Lloyd G, Lund V. Recurrence and its avoidance in juvenile angiofibroma. Laryngoscope 2001; 111: 1509–1511. doi:10.1097/00005537-200109000-00003.
[38] Kania RE, Sauvaget E, Guichard J-P, Chapot R, Huy PTB, Herman P. Early postoperative CT scanning for juvenile nasopharyngeal angiofibroma: detection of residual disease. AJNR Am J Neuroradiol 2005; 26: 82–88.
[39] d'Errico A, Pasian S, Baratti A, et al. A case-control study on occupational risk factors for sino-nasal cancer. Occup Environ Med 2009; 66: 448–455. doi:10.1136/oem.2008.041277.
[40] Bornholdt J, Hansen J, Steiniche T, et al. K-ras mutations in sinonasal cancers in relation to wood dust exposure. BMC Cancer 2008; 8: 53. doi:10.1186/1471-2407-8-53.
[41] Acheson ED, Cowdell RH, Hadfield E, Macbeth RG. Nasal cancer in woodworkers in the furniture industry. BMJ 1968; 2: 587–596. doi:10.1136/bmj.2.5605.587.
[42] Georgel T, Jankowski R, Henrot P, et al. CT assessment of woodworkers' nasal adenocarcinomas confirms the origin in the olfactory cleft. AJNR Am J Neuroradiol 2009; 30: 1440–1444. doi:10.3174/ajnr.A1648.
[43] Edge SB, Byrd DR. AJCC cancer staging manual. Springer; 2010.
[44] Cantù G, Bimbi G, Miceli R, et al. Lymph node metastases in malignant tumors of the paranasal sinuses: prognostic value and treatment. Arch Otolaryngol Head Neck Surg 2008; 134: 170–177.
[45] Boo H, Hogg JP. Nasal cavity neoplasms: a pictorial review. Curr Prob Diagn Radiol 2010; 39: 54–61. doi:10.1067/j.cpradiol.2009.07.001.
[46] Campo E, Harris NL, Jaffe ES, et al. WHO classification of tumours of haematopoietic and lymphoid tissue (IARC WHO classification of tumours). 4th ed. World Health Organization; 2008.
[47] Yen T-T, Wang R-C, Jiang R-S, Chen S-C, Wu S-H, Liang K-L. The diagnosis of sinonasal lymphoma: a challenge for rhinologists. Eur Arch Otorhinolaryngol 2012; 269: 1463–1469. doi:10.1007/s00405-011-1839-9.
[48] Ou C, Chen C, Ling J, Chai J. Nasal NK/T-cell lymphoma: computed tomography and magnetic resonance imaging findings.

J Chin Med Assoc. 2007; 70: 207–212. doi:10.1016/S1726-4901(09)70359-4.

[49] Lee FK-H, King AD, Ma BB-Y, Yeung DK-W. Dynamic contrast enhancement magnetic resonance imaging (DCE-MRI) for differential diagnosis in head and neck cancers. Eur J Radiol 2011; 81: 784–788. doi:10.1016/j.ejrad.2011 .01.089.

[50] Karantanis D, Subramaniam RM, Peller PJ, et al. The value of [(18)F]fluorodeoxyglucose positron emission tomography/computed tomography in extranodal natural killer/T-cell lymphoma. Clin Lymphoma Myeloma 2008; 8: 94–99. doi:10.3816/CLM.2008.n.010.

[51] Kim SJ, Oh SY, Hong JY, et al. When do we need central nervous system prophylaxis in patients with extranodal NK/T-cell lymphoma, nasal type? Ann Oncol 2010; 21: 1058–1063. doi:10.1093/annonc/mdp412.

[52] Gondivkar SM, Gadbail AR, Chole R, Parikh RV. Adenoid cystic carcinoma: a rare clinical entity and literature review. Oral Oncol 2011; 47: 231–236. doi:10.1016/j.oraloncology .2011.01.009.

[53] Menon S, Pai P, Sengar M, Aggarwal JP, Kane SV. Sinonasal malignancies with neuroendocrine differentiation: case series and review of literature. Indian J Pathol Microbiol 2010; 53: 28–34. doi:10.4103/0377-4929.59179.

[54] Rischin D, Coleman A. Sinonasal malignancies of neuroendocrine origin. Hematol/Oncol Clin North Am 2008; 22: 1297–1316. doi:10.1016/j.hoc.2008.08.008.

[55] Haas I, Ganzer U. Does sophisticated diagnostic workup on neuroectodermal tumors have an impact on the treatment of esthesioneuroblastoma? Onkologie 2003; 26: 261–267. doi:10.1159/000071622.

[56] Smith SR, Som P, Fahmy A, Lawson W, Sacks S, Brandwein M. A clinicopathological study of sinonasal neuroendocrine carcinoma and sinonasal undifferentiated carcinoma. Laryngoscope 2000; 110: 1617–1622. doi:10.1097/00005537-200010000-00007.

[57] Yoshioka H, Kamada T, Kandatsu S, et al. MRI of mucosal malignant melanoma of the head and neck. J Comput Assist Tomogr 1998; 22: 492–497. doi:10.1097/00004728-199805000-00024.

[58] Gal TJ, Silver N, Huang B. Demographics and treatment trends in sinonasal mucosal melanoma. Laryngoscope 2011; 121: 2026–2033.

[59] Haerle SK, Soyka MB, Fischer DR, et al. The value of (18)F-FDG-PET/CT imaging for sinonasal malignant melanoma. Eur Arch Otorhinolaryngol 2012; 269: 127–133. doi:10.1007/s00405-011-1664-1.